Intrinsic noise analysis and stochastic simulation on transforming growth factor beta signal pathway*

Wang Lu(王 路)[a)b)] and Ouyang Qi(欧阳颀)[a)b)†]

[a)] *The State Key Laboratory for Artificial Microstructures and Mesoscopic Physics, School of Physics, Peking University, Beijing* 100871, *China*

[b)] *Center for Theoretical Biology, Peking University, Beijing* 100871, *China*

(Received 21 April 2010; revised manuscript received 10 June 2010)

A typical biological cell lives in a small volume at room temperature; the noise effect on the cell signal transduction pathway may play an important role in its dynamics. Here, using the transforming growth factor-β signal transduction pathway as an example, we report our stochastic simulations of the dynamics of the pathway and introduce a linear noise approximation method to calculate the transient intrinsic noise of pathway components. We compare the numerical solutions of the linear noise approximation with the statistic results of chemical Langevin equations, and find that they are quantitatively in agreement with the other. When transforming growth factor-β dose decreases to a low level, the time evolution of noise fluctuation of nuclear Smad2–Smad4 complex indicates the abnormal enhancement in the transient signal activation process.

Keywords: transforming growth factor-β, noise, chemical Langevin equation, linear noise approximation

PACC: 8220F, 8725, 8730E

1. Introduction

Because a typical cell is on the order of only micrometers in linear size and it lives in room temperature environment, thermodynamic noise in a living cell may play an important role in the dynamics of its control system.[1−5] One of these effects is from the intrinsic noise of the dynamic system. As a result, the mean-field approximation, such as mass action law, used to study the dynamics of the cell behaviour may fail to reveal certain characteristics of the cell.[6−8] Here, using the transforming growth factor-β (TGF-β) signal pathway as an example, we point out that the general condition for such effects becomes important.

TGF-β signal pathway is essential to various aspects of cellular homeostasis, including proliferation, differentiation, migration and death.[9] As shown in Fig. 1(a), the major molecular events that comprise TGF-β signal transduction are initiated by binding ligands of TGF-β superfamily to TGF-β receptors to form the active signaling complex. Activated receptors phosphorylate receptor-regulated Smads, which form homomeric complexes and heteromeric complexes with Smad4. Then activated Smad complexes accumulate in the nucleus, where they directly regulate the transcription of target genes.[10−13] Malfunctions of TGF-β downstream signal are involved in serious human diseases, *inter alia*, many cancers, fibrosis, wound-healing disorders.[9,14,15]

Several mathematical models of TGF-β signal pathway have recently been published.[11,16−18] Most of them used deterministic ordinary differential equations (ODEs) to describe dynamical behaviours. Usually in these studies was also performed the sensitivity analysis on parameters. This kind of external perturbation to systematic parameters is also defined as external noise from parametric variations in a system.[4] However, the intrinsic noise in the signal transduction pathway has been rarely investigated.[1] To study the intrinsic noise, researchers start from the master equations, and usually use two approaches, i.e., the brute force numerical stochastic simulation such as Gillespie's stochastic simulation algorithm (SSA) or its derivatives, and the approximate methods.[19−21] Two frequently employed approximate methods are the chemical Langevin equations (CLEs) and the linear noise approximation (LNA).[3,4,21−26]

*Project supported by the National Natural Science Foundation of China (Grant No. 10721403), and the National Basic Research Program of China (Grant No. 2009CB918500).

†Corresponding author. E-mail: qi@pku.edu.cn

© 2010 Chinese Physical Society and IOP Publishing Ltd

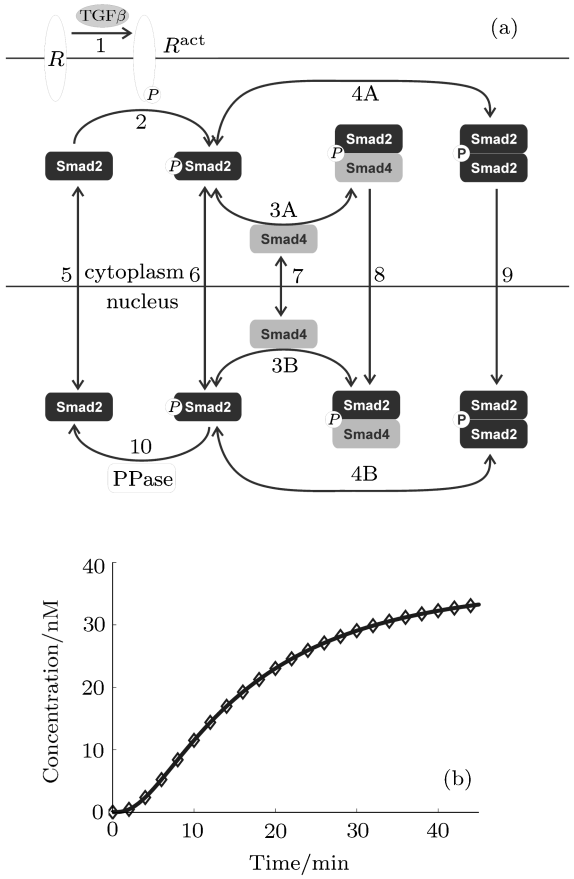


Fig. 1. Model scheme and time course of nuclear Smad2–Smad4 complex. Panel (a) shows the Smad activation and nucleocytoplasmic shuttling network used for modeling. Single-headed arrows indicate the irreversible reactions. Double-headed arrows indicate reversible reactions. Reaction 1 indicates the receptor activation by TGF-β binding. Reaction 2 indicates the irreversible phosphorylation of Smad2 by active receptor. Reactions 3A and 3B indicate the formation of cytoplasmic and nuclear Smad2–Smad4 complex. Reactions 4A and 4B indicate the formation of Smad2 homomeric complex in both the cytoplasm and the nucleus. Reactions 5 to 9 indicate the uni- or bi-direction shuttling of various Smad components between the cytoplasm and the nucleus, respectively. Reaction 10 indicates the dephosphorylation of phosphor-Smad2 by its phosphatases in the nucleus. Panel (b) exhibits the time course of nuclear Smad2–Smad4 complex, in which diamonds denote solution of CLEs, and solid line represents the deterministic solution of ODEs.

In the present work, we adopt the ODE model of the mass action law for TGF-β pathway recently developed by Schmierer *et al.*,[18] and perform the analysis on intrinsic noise by both CLEs and LNA. The results of numerical integral of LNA and stochastic simulations of CLEs are obtained and compared with each other.

2. Model and methodology

We adopt the simplified network of canonical TGF-β pathway in the work of Schmierer *et al.* (Fig. 1(a)).[18] The signal transduction is initiated by TGF-β activating its receptor on the cell surface. Then activated receptor phosphorylates cytoplasmic Smad2. Phosphorylated Smad2 forms homomeric complexes and heteromeric complexes with Smad4 in the cytoplasm and the nucleus reversibly. Unphosphorylated Smad2 and Smad4 constitutively shuttle between the cytoplasm and the nucleus. Since phosphorylated Smad2 and its homomeric and heteromeric complexes are actively transported into the nucleus with a higher rate than their constitutively shuttling, so the signaling causes them to accumulate predominantly in the nucleus. Phosphorylated Smad2 is irreversibly dephosphorylated by its phosphatase located in the nucleus. For further details of the ODE model see Appendix and Ref. [18].

In this system, quantitative experiments show that a number of key proteins are in a range of tens-of-thousand molecules per cell. The large number of molecules requires huge computational effort to perform the Gillespie's SSA. However, this situation probably satisfies the conditions of macroscopic infinitesimal time scale required for the Langevin approximation to be used.[23] Therefore, in this case the chemical Langevin equation will be a good approximation of SSA and enormously reduce the computational burden. We use the chemical Langevin equation approach based on the original ODE model to elucidate the influence of intrinsic noise.

Another approximate method recently used to investigate the intrinsic noise is the linear noise approximation, also called "system-size expansion", which was developed by Elf and Ehrenberg[22] and Kampen.[24] This method differs from the chemical Langevin equations in that it gives the information about intrinsic noise through repeating numerical simulation and data statistics. LNA deduces the explicit form of evolution equations of the variances, which depends on the numerical solution of original deterministic ODEs. For more details of the formulation of LNA, see Appendix and many other papers.[4,22,27,28]

3. Results

We converte the mean-field theory model of Schmierer *et al.*, and then converted it into CLE.[23]

The CLEs, which have the same initial values and parameters as the deterministic ODEs, are numerically solved by the Euler–Maruyama method. We repeat the stochastic simulation 100000 times and calculate the mean values of time course of the protein concentrations. As predicted, the mean values match well with the results of deterministic ODEs (Fig. 1(b)). Using CLEs, one can obtain the standard deviation of protein level by taking the same approach above. In the present work, we examine the results from LNA. Instead of solving stochastic integral of CLEs, LNA offers the deterministic ODEs of the variances of all components in the system, which can reduce much simulating time. The results of standard deviation are shown in Fig. 2. The numerical solutions of LNA perfectly accord with the statistic results of 100000 simulation runs of our CLEs. Because of continuous nucleocytoplasmic shuttling of Smad2, the intrinsic noises of cytoplasmic Smad2 and nuclear Smad2 are the same at time 0. The standard deviation of intrinsic noise is proportional to $\sqrt{N}$, where N is the total molecule number of this component. When the molecule number N increases, the noise usually increases as well; *vice versa*. The intrinsic noises of nuclear Smad2 and nuclear Smad2–Smad4 complexes monotonically follow the monotonic evolutions of their mean molecule numbers. However, when the mean molecule number of cytoplasmic Smad2 monotonically decreases (data not shown here), its fluctuation strength inversely increases in the first 10 min in TGF-β stimulation and then relaxes to a steady state (Fig. 2).

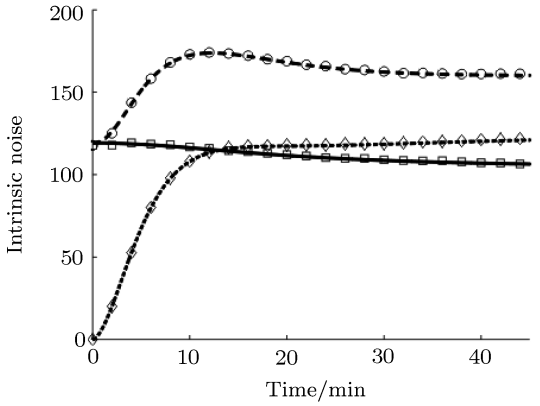


Fig. 2. Intrinsic noises of cytoplasmic and nuclear Smad2, and nuclear Smad2–Smad4 complex. The unit of intrinsic noise is molecule number. The intrinsic noise values for cytoplasmic Smad2 are denoted as dash line by LNA and circles by CLEs, for nuclear Smad2 as solid line by LNA and squares by CLEs, for nuclear Smad2–Smad4 complexes with dot line by LNA and diamonds by CLEs.

To test the effect of system volume on the intrinsic noise in the TGF-β signal transduction pathway, we define the signal-to-noise ratio (SNR) as the ratio of the mean molecule number to the standard deviation of its noise, and used the LNA to calculate the SNR of nuclear Smad2–Smad4 complex as a function of cell size. Nuclear Smad2–Smad4 complex is an active complex for the transcription of target genes and plays a key role in the TGF-β signal transduction pathway. The total volume in the original paper of Schmierer *et al.* was about 3.3×10^{-12} L corresponding to around 9.2-μm radius (r_0), with assuming the cell to be ball-shaped. Besides the original volume, we calculate SNRs for three other conditions: 1/5 r_0, 1/10 r_0 and 1/20 r_0 (Fig. 3). We assume that the total molecules of all components in the system, except TGF-β receptor, change in the same proportion as the volume does, thus its initial concentration is kept unchanged as its original value. We further assume that the number of TGF-β receptor molecule is proportional to the area of cell surface, or the square of radius. Therefore, cell with a smaller volume has a higher ratio of the receptor density to the concentrations of other molecules. In addition, we kept the same TGF-β level for all conditions. Generally, in the steady state the SNR of nuclear Smad2–Smad4 complex goes up with the increase of system size and molecule number. The signal-to-noise ratio is above 200 so that the intrinsic noise is not obvious in the original cell volume.

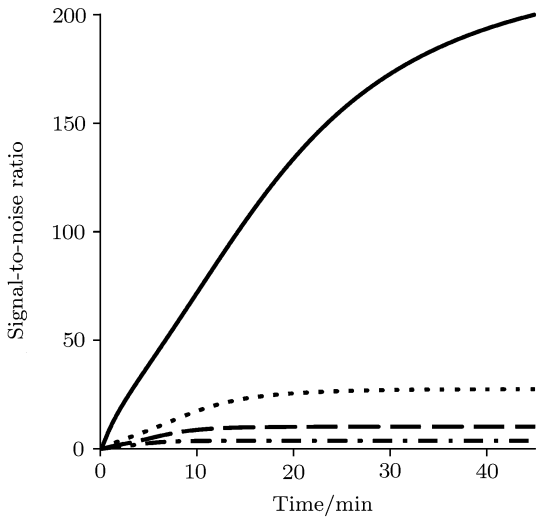


Fig. 3. Signal-to-noise ratios of nuclear Smad2–Smad4 complex for different system sizes. Solid line denotes original radius (r_0), dot line 1/5 r_0, dash line 1/10 r_0, dash-dot line 1/20 r_0.

However, if the cell size reduces to one micrometer level, the ratio of signal to noise reduces to about 3,

and it becomes quite important for the transcription of target genes.

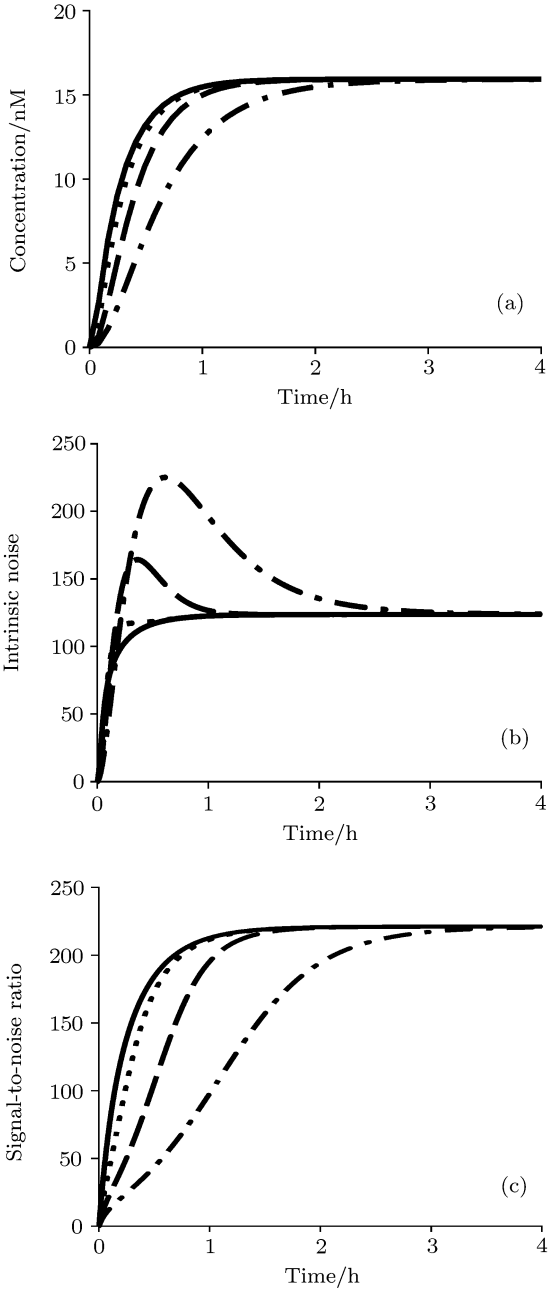


Fig. 4. Dependences of intrinsic noise of nuclear Smad2–Smad4 complex on TGF-β concentrations. Dot line denotes results for the original TGF-β concentration (c_0), solid line for 3-fold of c_0, dash line for 1/3 c_0, dash dot line for 1/9 c_0. Panel (a) shows the time course of nuclear Smad2–Smad4 complex concentration, panel (b) the time course of intrinsic noise of nuclear Smad2–Smad4 complex, panel (c) the signal-to-noise ratio of nuclear Smad2–Smad4 complex.

Finally, we simulate the time courses of nuclear Smad2–Smad4 complex ($S24n$) under different dose levels of TGF-β (Fig. 4). As in our simple model is considered only the short-term activation process, the degradation of proteins is not included. And the binding of TGF-β to its receptor is irreversible, thus the final steady state of $S24n$ is determined only by the total receptor level, even if the dose of TGF-β changes (Fig. 4(a)). Although TGF-β varies 27-fold, the transient behaviour of $S24n$ does not change qualitatively (Fig. 4(a)). The process that protein level reaches half the maximum under the lowest TGF-β level delays about half an hour in comparison with the highest TGF-β level. However, the standard deviations of $S24n$ in Fig. 4(b) show that they are obviously different. As for the highest TGF-β level, the intrinsic noise monotonically increases to the steady-state level with protein concentration increasing. However, the curve corresponding to the lower TGF-β stimulation shows that the intrinsic noise first overshoots and then relaxes to a steady state, which indicates that other reactions or processes significantly enhance the fluctuation of $S24n$ in the first 2 h. The maximum level of intrinsic noise appears around 40 min after TGF-β signaling, and is almost as 2-fold high as the steady-state level. At the same time (40 min), the concentration of $S24n$ is apparently lower than that under the higher TGF-β levels. The signal-to-noise ratio of $S24n$ at the lowest TGF-β level is much lower than that at high TGF-β level during the first hour stimulation (Fig. 4(c)). Since $S24n$ serves as a key activator of downstream gene transcription, the apparent increase of its intrinsic noise can have a remarkable influence on cell fate when the total number of proteins is low.

4. Conclusions

In this work, we have investigated the intrinsic noise in TGF-β signal pathway. The noise is calculated based on the linear noise approximation method of chemical master equation and compared with the simulating statistics of chemical Langevin equations. In the CLEs are used the normal random variables to approximate Poisson random variables in the real process.[23] In the LNA is utilized the truncated Taylor series to approximate the chemical master equations, and linear Fokker–Planck equations which have a Gaussian-form solution are obtained.[24] Therefore the results of LNA quantitatively correspond to those of CLEs. The deterministic ODEs of component variances derived from the LNA offer a useful tool for noise analysis, and it is a good substitute for CLEs to calculate the transient evolution of intrinsic noise. The LNA can save much simulating time in comparison with stochastic simulation methods. In addition, it is noticeable that the LNA is used to calculate the variance based on the deterministic solution of ODEs.

Therefore the LNA ignores the interaction between the mean (the first moment) and the variance (the second moment) of protein level, and is also inappropriate to describe the near-critical phenomena.[27,29]

In many biological systems, especially the unicellular prokaryotes and eukaryotes whose system sizes are rather small, the intrinsic noise plays an important role in regulating gene expression and signal transduction.[1,3,30] The SNR calculation indicates that since the mammalian cells usually are much larger than the unicellular organisms, and the number of individual proteins often reaches tens of thousands in the mammalian cells, therefore in this kind of system the intrinsic noise is negligible in the most cases. In our simple model of TGF-β signal pathway, our results indicate that the intrinsic noise shows transient enhancement when external TGF-β stimulus decreases. The transient amplification of intrinsic noise can cause significant downstream effects and induce distinct cellular responses. More attention should be paid to the influence of intrinsic noise on signal transduction pathway in the future research.

Appendix

(i) ODEs and parameters adopted from the work of Schmierer *et al.*[18] The concentration unit of all component is nM. The meanings of variables and parameters are shown in Tables 1 and 2.

Table 1. Initial number of proteins at time=0. All initial conditions are cited from the original model file given by Schmierer *et al.*[18]

symbol	biological meaning	compartment	concentration, nM	particle number
TGF-β			0.0659	
R	TGF- β receptor	cytoplasm	1.025	1400
R^{act}	active receptor	cytoplasm	0	0
$S2c$	Smad2/3	cytoplasm	60.64	82840
$S2n$	Smad2/3	nucleus	28.49	17160
$S4c$	Smad4	cytoplasm	50.81	69400
$S4n$	Smad4	nucleus	50.81	30600
$pS2c$	phospho–$S2c$	cytoplasm	0	0
$pS2n$	Phospho–$S2c$	nucleus	0	0
$S22c$	$pS2c$–$pS2c$ complex	cytoplasm	0	0
$S22n$	$pS2n$–$pS2n$ complex	nucleus	0	0
$S24c$	$pS2c$–$S4c$ complex	cytoplasm	0	0
$S24n$	$pS2n$–$S4n$ complex	nucleus	0	0
PP	phosphatase	nucleus	0.996	600

$$
\begin{aligned}
&\frac{\mathrm{d}}{\mathrm{d}t}R = -k_{TGF\beta}\cdot R\cdot TGF\beta,\\
&\frac{\mathrm{d}}{\mathrm{d}t}R^{\mathrm{act}} = k_{TGF\beta}\cdot R\cdot TGF\beta,\\
&\frac{\mathrm{d}}{\mathrm{d}t}S2c = \frac{k_{\mathrm{ex}}\cdot S2n}{CNR} - k_{\mathrm{in}}\cdot S2c - k_{phos}\cdot S2c\cdot R^{\mathrm{act}},\\
&\frac{\mathrm{d}}{\mathrm{d}t}pS2c = \frac{k_{\mathrm{ex}}\cdot pS2n}{CNR} - k_{\mathrm{in}}\cdot pS2c + k_{phos}\cdot S2c\cdot R^{\mathrm{act}}\\
&\qquad\qquad - k_{\mathrm{on}}\cdot pS2c\cdot(S4c + 2\cdot pS2c) + k_{\mathrm{off}}\cdot(S24c + 2\cdot S22c),\\
&\frac{\mathrm{d}}{\mathrm{d}t}S4c = k_{\mathrm{in}}\cdot S4n - k_{\mathrm{in}}\cdot S4c - k_{\mathrm{on}}\cdot S4c\cdot pS2c + k_{\mathrm{off}}\cdot S24c,\\
&\frac{\mathrm{d}}{\mathrm{d}t}S24c = k_{\mathrm{on}}\cdot S4c\cdot pS2c - k_{\mathrm{off}}\cdot S24c - k_{\mathrm{in}}\cdot CIF\cdot S24c,\\
&\frac{\mathrm{d}}{\mathrm{d}t}S22c = k_{\mathrm{on}}\cdot pS2c^2 - k_{\mathrm{off}}\cdot S22c - k_{\mathrm{in}}\cdot CIF\cdot S22c,\\
&\frac{\mathrm{d}}{\mathrm{d}t}S2n = k_{\mathrm{in}}\cdot S2c\cdot CNR - k_{\mathrm{ex}}\cdot S2n + k_{\mathrm{de}}\cdot pS2n\cdot PP,
\end{aligned}
$$

$$\frac{\mathrm{d}}{\mathrm{d}t}pS2n = k_{\mathrm{in}} \cdot pS2c \cdot CNR - k_{\mathrm{ex}} \cdot pS2n - k_{\mathrm{de}} \cdot pS2n \cdot PP - k_{\mathrm{on}} \cdot pS2n \cdot (S4n + 2 \cdot pS2n) + k_{\mathrm{off}} \cdot (S24n + 2 \cdot S22n),$$

$$\frac{\mathrm{d}}{\mathrm{d}t}S4n = k_{\mathrm{in}} \cdot S4c \cdot CNR - k_{\mathrm{in}} \cdot S4n \cdot CNR - k_{\mathrm{on}} \cdot S4n \cdot pS2n + k_{\mathrm{off}} \cdot S24n,$$

$$\frac{\mathrm{d}}{\mathrm{d}t}S24n = k_{\mathrm{on}} \cdot S4n \cdot pS2n - k_{\mathrm{off}} \cdot S24n + k_{\mathrm{in}} \cdot CIF \cdot S24c \cdot CNR,$$

$$\frac{\mathrm{d}}{\mathrm{d}t}S22n = k_{\mathrm{on}} \cdot pS2n^2 - k_{\mathrm{off}} \cdot S22n + k_{\mathrm{in}} \cdot CIF \cdot S22c \cdot CNR.$$

Table 2. Parameter values in the model. All parameters are cited from the original model file given by Schmierer *et al.*[18]

symbol	biological meaning	value	unit	reaction No.
$k_{TGF\beta}$	receptor activation rate by TGF-β	$7.41{\cdot}10^{-2}$	$\mathrm{nM}^{-1}{\cdot}\mathrm{s}^{-1}$	1
k_{phos}	Smad2 phosphorylation rate	$4.04{\cdot}10^{-4}$	$\mathrm{nM}^{-1}{\cdot}\mathrm{s}^{-1}$	2
k_{on}	association rate for Smad complex	$1.84{\cdot}10^{-3}$	$\mathrm{nM}^{-1}{\cdot}\mathrm{s}^{-1}$	3A, 3B, 4A, 4B
k_{off}	dissociation rate for Smad complex	$1.6{\cdot}10^{-2}$	s^{-1}	3A, 3B, 4A, 4B
k_{in}	nuclear import rate	$2.61{\cdot}10^{-3}$	s^{-1}	5, 6, 7, 8, 9
k_{ex}	nuclear export rate	$1.26{\cdot}10^{-2}$	s^{-1}	5, 6, 7
k_{de}	pSmad2 dephosphorylation rate	$6.57{\cdot}10^{-3}$	$\mathrm{nM}^{-1}{\cdot}\mathrm{s}^{-1}$	10
CIF	complex import factor	5.7	–	8, 9
V_{cyt}	cytoplasmic volume	$2.268{\cdot}10^{-12}$	L	
V_{nuc}	nuclear volume	$1{\cdot}10^{-12}$	L	
CNR	ratio of V_{cyt} to V_{nuc}	2.268	–	

(ii) Linear noise approximation

The LNA is a power series expansion of the master equation in the system size Ω. In the volume Ω, the number of molecules is approximately expressed as

$$X_i = \Omega c_i + \sqrt{\Omega}\alpha_i, \tag{A1}$$

where X_i is the copy number of component $i = 1, 2, \ldots, N$; c_i is its macroscopic concentration defined as $c_i = \lim_{\Omega\to\infty} X_i/\Omega$; α_i is a new random variable describing the deviation from c_i. The macroscopic system dynamics is described by N deterministic ODEs as follows:

$$\frac{\mathrm{d}}{\mathrm{d}t}\boldsymbol{c} = f(\boldsymbol{c}) = \boldsymbol{S} \cdot \boldsymbol{v}, \tag{A2}$$

where $\boldsymbol{c} = (c_1, c_2, \ldots, c_N)^{\mathrm{T}}$, $\boldsymbol{S}$ is the stoichiometry matrix, $\boldsymbol{v}$ is the velocity vector that contains R reactions. The master equation for the probability $P(X, t)$ with $\boldsymbol{X} = (X_1, X_2, \ldots, X_N)^{\mathrm{T}}$ is

$$\frac{\mathrm{d}}{\mathrm{d}t}P(\boldsymbol{X}, t) = \Omega \sum_{j=1}^{R} \left(\prod_{i=1}^{N} E_i^{-S_{ij}} - 1 \right) \cdot v_j(x, \Omega) \cdot P(\boldsymbol{X}, t), \tag{A3}$$

where S_{ij} is the (i, j) element of $\boldsymbol{S}$, $E_i^{-S_{ij}}$ is the step operator with the property that $E_i^k f(\ldots, X_i, \ldots) = f(\ldots, X_i + k, \ldots)$, v_j is the j element of $\boldsymbol{v}$.

The step operator E_i^k changes X_i into $X_i + k$ and increases the value of α_i by $k/\sqrt{\Omega}$. Thus, for a large system volume, a single reaction brings about a small concentration change and the operator E_i^k is approximated by a truncated Taylor series of differential operator as follows:

$$E_i^k \approx 1 + \frac{k}{\sqrt{\Omega}}\frac{\partial}{\partial\alpha_i} + \frac{k^2}{2\Omega}\frac{\partial^2}{\partial\alpha_i^2}. \tag{A4}$$

For operation in several dimensions one obtains

$$E^{-S_{\cdot j}} = \prod_{i=1}^{N} E_i^{-S_{ij}} \approx 1 - \frac{1}{\sqrt{\Omega}} \sum_{i=1}^{N} S_{ij}\frac{\partial}{\partial\alpha_i} + \frac{1}{2\Omega} \sum_{i,k=1}^{N} S_{ij}S_{kj}\frac{\partial^2}{\partial\alpha_i\partial\alpha_k}. \tag{A5}$$

As $\boldsymbol{X} = \Omega\boldsymbol{c} + \sqrt{\Omega}\boldsymbol{\alpha}$, the probability distribution $\theta(\boldsymbol{\alpha}, t)$ is related to $P(\boldsymbol{X}, t)$ by

$$P(\boldsymbol{X}, t) = P(\Omega\boldsymbol{c} + \sqrt{\Omega}\boldsymbol{\alpha}, t) = \theta(\boldsymbol{\alpha}, t). \tag{A6}$$

Therefore

$$\frac{\mathrm{d}}{\mathrm{d}t}P(\boldsymbol{X}, t) = \frac{\partial}{\partial t}\theta(\boldsymbol{\alpha}, t) - \sqrt{\Omega}\sum_{i=1}^{N}\frac{\mathrm{d}}{\mathrm{d}t}c_i\frac{\partial}{\partial\alpha_i}\theta(\boldsymbol{\alpha}, t). \tag{A7}$$

Taylor expansion of the velocity vector $\boldsymbol{v}$ around the macroscopic concentration $\boldsymbol{c}$ is

$$v_i(\boldsymbol{X},\Omega) \approx v_i(\boldsymbol{c}) + \frac{1}{\sqrt{\Omega}} \sum_{i=1}^{N} \frac{\partial v_i(\boldsymbol{c})}{\partial c_i} \alpha_i. \tag{A8}$$

Equations (A5)–(A8) are inserted into the master equation (A3), and then Ω terms with the same order are collected (see Ref. [24] for details). The term of order $\Omega^{1/2}$ corresponds to the macroscopic rate equation (A2). The term of order Ω^0 yields the general form of a multivariate linear Fokker–Planck equation, which governs the evolution of $\theta(\boldsymbol{\alpha}, t)$ as follows:

$$\frac{\partial}{\partial t}\theta(\boldsymbol{\alpha},t) = -\sum_{i,k=1}^{N} A_{ik} \frac{\partial}{\partial \alpha_i}(\alpha_k \theta) + \frac{1}{2} \sum_{i,k=1}^{N} B_{ik} \frac{\partial^2}{\partial \alpha_i \partial \alpha_k}\theta, \tag{A9}$$

where $A_{ik} = \left.\dfrac{\partial(\boldsymbol{S}\cdot\boldsymbol{v})_i}{\partial c_k}\right|_{c(t)}$ are the elements of Jacobian matrix $\boldsymbol{A}$, and

$$B_{ik} = \sum_{j=1}^{R} S_{ij} S_{kj} v_j = [\boldsymbol{S}\cdot \mathrm{diag}(\boldsymbol{v})\cdot \boldsymbol{S}]_{ik}$$

are the elements of the diffusion matrix $\boldsymbol{B}$. We use this equation to determine the evolution equations of the means $\langle \alpha_i \rangle$ and the variances $\langle (\alpha_i - \langle \alpha_i \rangle)(\alpha_j - \langle \alpha_j \rangle) \rangle$ by being multiplied with α_i and being integrated over all α's. For the means, we obtain the following equation:

$$\frac{\mathrm{d}}{\mathrm{d}t} \langle \boldsymbol{\alpha} \rangle = \boldsymbol{A} \langle \boldsymbol{\alpha} \rangle . \tag{A10}$$

If we assume that the initial state is accurately determined, then $\langle \boldsymbol{\alpha}(0) \rangle = 0$and the means $\langle \boldsymbol{\alpha}(t) \rangle$ will keep zero at all times. For the variance matrix $\boldsymbol{C} = \langle \boldsymbol{\alpha}\boldsymbol{\alpha}^{\mathrm{T}} \rangle$, we obtain a set of ODEs that determine the variances and the covariance of the fluctuations of $\boldsymbol{X}$, which can be written in matrix-vector form as follows:

$$\frac{\mathrm{d}}{\mathrm{d}t}\boldsymbol{C} = \boldsymbol{A}\boldsymbol{C} + \boldsymbol{C}\boldsymbol{A}^{\mathrm{T}} + \boldsymbol{B}. \tag{A11}$$

The coefficient matrices $\boldsymbol{A}$ and $\boldsymbol{B}$ are time-dependent and independent of fluctuation $\boldsymbol{\alpha}$.

Acknowledgement

We thank H. L. Wang and L. Yan for their helpful discussions.

References

[1] Wang H L, Fu Z P, Xu X H and Ouyang Q 2009 *Chin. Phys.* B **18** 2082
[2] Bezrukov S M and Vodyanoy I 1995 *Nature* **378** 362
[3] Elowitz M B, Levine A J, Siggia E D and Swain P S 2002 *Science* **297** 1183
[4] Scott M, Ingalls B and Kaern M 2006 *Chaos* **16** 026107
[5] Li Z Y, Xie Z W, Chen T and Ouyang Q 2009 *Chin. Phys.* B **18** 5544
[6] Heinrich R, Neel B G and Rapoport T A 2002 *Mol. Cell* **9** 957
[7] Raser J M and O'Shea E K 2005 *Science* **309** 2010
[8] Eissing T, Allgower F and Bullinger E 2005 *Syst. Biol. (Stevenage)* **152** 221
[9] Massague J 2008 *Cell* **134** 215
[10] Shi Y and Massague J 2003 *Cell* **113** 685
[11] Clarke D C and Liu X 2008 *Trends Cell Biol.* **18** 430
[12] Hill C S 2009 *Cell Res.* **19** 36
[13] Schmierer B and Hill C S 2005 *Mol. Cell. Biol.* **25** 9845
[14] Howell J E and McAnulty R J 2006 *Curr. Drug. Targets* **7** 547
[15] Schiller M, Javelaud D and Mauviel A 2004 *J. Dermatol. Sci.* **35** 83
[16] Chung S W, Miles F L, Sikes R A, Cooper C R, Farach-Carson M C and Ogunnaike B A 2009 *Biophys. J.* **96** 1733
[17] Nakabayashi J and Sasaki A 2009 *J. Theor. Biol.* **259** 389
[18] Schmierer B, Tournier A L, Bates P A and Hill C S 2008 *Proc. Nat. Acad. Sci. USA* **105** 6608
[19] Gillespie D T 1977 *J. Phys. Chem.* **81** 2340
[20] Rathinam M, Petzold L R, Cao Y and Gillespie D T 2003 *J. Chem. Phys.* **119** 12784
[21] Gardiner C W 1985 *Handbook of Stochastic Methods for Physics, Chemistry, and the Natural Sciences* (Berlin, New York: Springer-Verlag) Chap. 7
[22] Elf J and Ehrenberg M 2003 *Genome Res.* **13** 2475
[23] Gillespie D T 2000 *J. Chem. Phys.* **113** 297
[24] Kampen N G V 1992 *Stochastic Processes in Physics and Chemistry* (Amsterdam, New York: North-Holland) Chap. 10
[25] Ullah M and Wolkenhauer O 2007 *IET Syst. Biol.* **1** 247
[26] Chen A M, Zhang J J, Yuan Z J and Zhou T S 2009 *Acta Phys. Sin.* **58** 2804 (in Chinese)
[27] Elf J, Paulsson J, Berg O G and Ehrenberg M 2003 *Biophys. J.* **84** 154
[28] Yan L, Wang H L and Ouyang Q 2010 *Chin. Phys. Lett.* **27** 010501
[29] Ullah M and Wolkenhauer O 2010 *Wiley Interdisciplinary Reviews: Systems Biology and Medicine* Advance access published on December 10, 2009; doi:10.1002/wsbm.078.
[30] Thattai M and van Oudenaarden A 2001 *Proc. Nat. Acad. Sci. USA* **98** 8614